DMD Fast Forward. Published on February 23, 2022 as DOI: 10.1124/dmd.121.000624
This article has not been copyedited and formatted. The final version may differ from this version.

CYP2C19 plays a major role in the hepatic *N*-oxidation of cotinine

Yadira X. Perez-Paramo[1,2], Christy J.W. Watson[1], Gang Chen[1], Philip Lazarus[1]

[1]Department of Pharmaceutical Sciences, College of Pharmacy and Pharmaceutical Sciences, Washington State University, Spokane, Washington, USA

Corresponding author: Philip Lazarus, PhD, Department of Pharmaceutical Sciences, PBS 323, Washington State University College of Pharmacy and Pharmaceutical Sciences, 412 E. Spokane Falls Blvd.
Spokane, WA, USA, 99202-2131; e-mail: phil.lazarus@wsu.edu

[2]**Current affiliation:** Genentech, Inc., South San Francisco, California, USA 94080

DMD Fast Forward. Published on February 23, 2022 as DOI: 10.1124/dmd.121.000624
This article has not been copyedited and formatted. The final version may differ from this version.

Running title: CYP2C19 variants and cotinine-*N*-oxide metabolism

Number of text pages:

Number of tables: 2

Number of figures: 4

Number of references: 78

Supplemental: 2 figures, 3 tables

Number of words:

Abstract: 230 words

Introduction: 643 words

Discussion: 1,028 words

Abbreviations: 3HC, 3-hydroxy cotinine; CEU, Northern Europeans from Utah; COT, cotinine; COT-Gluc, cotinine-*N*- glucuronide; CPIC, Clinical Pharmacogenetics Implementation Consortium; COX, cotinine-*N*-oxide; CYP, cytochrome P450; EM, extensive metabolizers; ESI, electrospray ionization; FMO, flavin monooxygenase; HEK293, human embryonic kidney 293 cells; HLM, human liver microsomes; HRP, horseradish peroxidase; IM, intermediate metabolizers; K_M, Michaelis constant; MAF, minor allele frequency; MRM; multiple reaction monitoring; NADPH, nicotinamide adenine dinucleotide phosphate; NMR, nicotine metabolic ratio; PM, poor metabolizers; SAF, skin autofluorescence; SDS, sodium dodecyl sulfate; SNP, single nucleotide

DMD Fast Forward. Published on February 23, 2022 as DOI: 10.1124/dmd.121.000624
This article has not been copyedited and formatted. The final version may differ from this version.

polymorphisms; UGT, uridine 5'-diphospho-glucuronosyltransferase; UM, ultra-rapid metabolizers; UHPLC-MS/MS, ultra-high pressure liquid chromatography-mass spectrometry; V_{max}, maximum reaction rate.

DMD Fast Forward. Published on February 23, 2022 as DOI: 10.1124/dmd.121.000624
This article has not been copyedited and formatted. The final version may differ from this version.

Abstract

The major mode of metabolism of nicotine is via the formation of cotinine by the enzyme cytochrome P450 (CYP) 2A6. Cotinine undergoes further CYP2A6-mediated metabolism by hydroxylation to 3-hydroxycotinine and norcotinine but can also form cotinine-*N*-glucuronide and cotinine-*N*-oxide (COX). The goal of the present study was to investigate the enzymes that catalyze COX formation and determine whether genetic variation in these enzymes may affect this pathway. Specific inhibitors of major hepatic cytochrome P450 (CYP) enzymes were used in cotinine-*N*-oxidation reactions using pooled human liver microsomes (HLM). COX formation was monitored by ultra-high pressure liquid chromatography-mass spectrometry and enzyme kinetic analysis was performed using microsomes from CYP-overexpressing HEK293 cell lines. Genotype-phenotype analysis was performed in a panel of 113 human liver specimens. Inhibition of COX formation was only observed in HLM when using inhibitors of CYPs 2A6, 2B6, 2C19, 2E1, and 3A4. Microsomes from cells overexpressing CYPs 2A6 or 2C19 exhibited similar *N*-oxidation activity against cotinine, with V_{max}/K_M values of 4.4 and 4.2 nL/min/mg, respectively. CYP2B6-, CYP2E1-, and CYP3A4-overexpressing microsomes were also active in COX formation. Significant associations ($p<0.05$) were observed between COX formation and genetic variants in CYPs 2C19 (*2 and *17 alleles) in HLM. These results demonstrate that genetic variants in CYP2C19 are associated with decreased COX formation, potentially affecting the relative levels of cotinine in the plasma or urine of smokers and ultimately affecting recommended smoking cessation therapies.

DMD Fast Forward. Published on February 23, 2022 as DOI: 10.1124/dmd.121.000624
This article has not been copyedited and formatted. The final version may differ from this version.

Significance Statement

This study is the first to elucidate the enzymes responsible for cotinine-*N*-oxide formation and genetic variants that affect this biological pathway. Genetic variants in CYP2C19 have the potential to modify NMR in smokers and could affect pharmacotherapeutic decisions for smoking cessation treatments.

DMD Fast Forward. Published on February 23, 2022 as DOI: 10.1124/dmd.121.000624
This article has not been copyedited and formatted. The final version may differ from this version.

Introduction

The major mode of metabolism of nicotine in smokers (~ 70%) is via the formation of cotinine (COT) by the cytochrome P450 (CYP) enzyme, 2A6. COT is slowly eliminated from plasma with a half-life of 10-27 h (Jarvis et al., 1988), undergoing metabolism by hydroxylation to 3-hydroxy-COT (3HC) (Miki et al., 1996) and *N*-(hydroxyl-methyl) norcotinine (Brown et al., 2005), glucuronidation to cotinine-*N*-glucuronide (COT-Gluc) (Chen et al., 2007), and oxidation to COT-*N*-oxide (COX), accounting for an average of 63, 4, 24, and 9% of cotinine metabolites, respectively, in the urine of Caucasian smokers (Figure 1) (Rangiah et al., 2011). While extensive studies have been performed examining the enzymes responsible for the formation of COT (Miki et al., 1996), *N*-(hydroxymethyl)-norcotinine (Brown et al., 2005), and COT-Gluc (Chen et al., 2010), no studies have identified the enzymes responsible for COX formation (Yamanaka et al., 2004; Yildiz, 2004).

Potentially, an important role for COX may be as a factor that affects the Nicotine Metabolic Ratio (NMR), which describes the ratio of plasma 3HC to COT in individual smokers (Dempsey et al., 2004), as a biomarker of nicotine addiction. This ratio is highly correlated with nicotine clearance in humans and has been generally accepted as an *in vivo* marker for CYP2A6 activity (Dempsey et al., 2004). The NMR is widely used to assess nicotine dependence and smoking behavior (Falcone et al., 2011), and to aid clinicians in the most efficacious pharmacotherapy for smoking cessation (Chen et al., 2018; Lerman et al., 2006, 2015; Malaiyandi et al., 2006). It has been shown that the NMR is highly variable among different demographic groups and that these differences

DMD Fast Forward. Published on February 23, 2022 as DOI: 10.1124/dmd.121.000624
This article has not been copyedited and formatted. The final version may differ from this version.

could be affecting smoking cessation rates at the population level (Baurley et al., 2016; Fix et al., 2017). It has also been widely reported that nicotine metabolism varies among patients and that some of this variation can be explained by genetic variation in genes involved in the nicotine metabolism pathway (Chenoweth et al., 2014; Hukkanen et al., 2005). While alterations in the levels of 3HC-Gluc did not affect the NMR in African American subjects regardless of UGT2B17 genotype (Zhu et al., 2013), it was reported that the NMR is influenced by the levels of COT-Gluc formation in both Caucasian and African American smokers (Berg et al., 2010; Jacobson & Ferguson, 2014; Murphy et al., 2014, 2017) and variability in NMR due to differences in COT-Gluc formation were suggested to be of particular importance in populations with a high prevalence of functional UGT2B10 genetic variants (e.g., African Americans) (Murphy, 2017).

The presence of COX was first reported by Dagne *et al* in male rhesus monkey urine in 1972 (Dagne & Castagnoli, 1972)**.** Recent evidence has suggested that urinary COX is an effective biomarker of the effects of environmental or second hand tobacco smoking on skin autofluorescence (SAF), a tool used to predict diabetes-related cardiovascular complications (Van Waateringe et al., 2017). COX has also been used as a biomarker for active nicotine consumption in athletes (Marclay et al., 2011) and as a biomarker of nicotine exposure in breast milk (Pellegrini et al., 2007). Studies examining the potential role of the flavin monooxygenase (FMO) enzymes demonstrated that none of these enzymes exhibited COX formation activity (Gorrod & Peyton, 1999; Tsai & Gorrod, 1999). Additional studies using CYP450 inhibitors demonstrated that COX is formed from COT in hamster and guinea pig liver microsomes, potentially by CYP450 enzymes (Jenner et al., 1971). This was validated

DMD Fast Forward. Published on February 23, 2022 as DOI: 10.1124/dmd.121.000624
This article has not been copyedited and formatted. The final version may differ from this version.

in further studies where phenobarbital (a strong CYP450 inducer) pretreatment in rat liver increased COX production by 8-fold, an effect that was negated when co-treated with the CYP450 inhibitor, metyrapone (Foth et al., 1992). The goal of the present study was to identify the human CYP450 enzymes responsible for COX formation and to determine whether genetic variations in these enzymes affect the levels of COX formation in a panel of human liver specimens.

DMD Fast Forward. Published on February 23, 2022 as DOI: 10.1124/dmd.121.000624
This article has not been copyedited and formatted. The final version may differ from this version.

Materials and Methods

Chemicals and Materials. Dulbecco's Modified Eagles Medium, Dulbecco's phosphate-buffered saline, fetal bovine serum, and geneticin (G418) were purchased from Gibco (Grand Island, New York, USA). Anti-V5-HRP antibody, was obtained from Invitrogen (Carlsbad, California, USA) while the anti-calnexin-HRP antibody was purchased from Abcam (Cambridge, UK). The BCA protein assays used for total protein quantification were purchased from Pierce (Rockford, Illinois, USA) and the NADPH regeneration system was purchased from Corning (Corning, New York, USA). The following chemicals used for *in vitro N*-oxidation activity assays were purchased from Sigma Aldrich (St. Louis, Missouri, USA): phenacetin, bupropion, amodiaquine, diclofenac, omeprazole, dextromethorphan, chlorzoxazone, midazolam, furafylline, clopidogrel, montelukast, sulfaphenazole, tranylcypromine, quinidine, clomethiazole, ketoconazole, and cotinine. Pooled HLM were purchased from Sekisui XenoTech (Kansas City, Kansas, USA) while pooled human liver RNA was purchased from Biochain (Newark, CA). SuperScript VILO synthesis kit was purchased from Thermo Fisher Scientific (Waltman, MA) and TaqMan probes were purchased from AB Applied Biosystems (Foster City, CA, USA). High performance liquid chromatography-grade ammonium acetate and acetonitrile were purchased from Fisher Scientific (Pittsburgh, Pennsylvania, USA) while the ACQUITY UPLC BEH-HILIC (1.7µm 2.1 x 100 mm) column was purchased from Waters (Milford, Massachusetts, USA). Cotinine, COX, 3HC as well as the internal standards D_3-COX and D_3-3HC were purchased from Toronto Research Chemicals (Ontario, Canada).

DMD Fast Forward. Published on February 23, 2022 as DOI: 10.1124/dmd.121.000624
This article has not been copyedited and formatted. The final version may differ from this version.

Biological specimens. Normal human liver specimens and matching genomic DNA samples from 113 subjects were provided by the Tissue Procurement Facility at the H. Lee Moffitt Cancer Center (Tampa, FL) as previously described (Coughtrie et al., 1987; Yokota et al., 1989). All subjects were Caucasian, 43% (n=47) were female, and the mean age of the subjects was 64 y. Microsomes were prepared as described previously and were stored at -80^{o}C (Chen et al., 2012). All protocols involving tissue specimens were approved by the institutional review board at the H. Lee Moffitt Cancer Center and in accordance with assurances filed with and approved by the United States Department of Health and Human Services.

CYP inhibition assays in HLM. Inhibition reactions (final volume = 25 µL) contained 25 µg of total pooled HLM protein, 50 mM potassium phosphate, NADPH regenerating system (1.55 mmol/L NADP+, 3.3 mmol/L glucose-6-phosphate, 3.3 mmol/L $MgCl_2$, and 0.5 U of 40 U/mL glucose-6-phosphate dehydrogenase), and 500 µM COT. Specific CYP inhibitors were added at concentrations of 1 or 10 µM: furafylline [CYP1A2; (Sesardic et al., 1990)], tranylcypromine [CYP2A6 and CYP2C19; (Draper et al., 1997; Taavitsainen et al., 2001)], clopidogrel [CYP2B6; (Richter et al., 2004)], montelukast [CYP2C8; (Walsky et al., 2005)], sulfaphenazole [CYP2C9; (Miners et al., 1988)], quinidine [CYP2D6; (von Bahr et al., 1985)], clomethiazole [CYP2E1; (Stresser et al., 2016)], or ketoconazole [CYP3A4; (Maurice et al., 1992)] (see Supp. Table 1). All reactions were incubated for 30 min at 37°C, with reactions terminated by the addition of 25 µL ice-cold acetonitrile containing 0.001 ppm internal standard (D_3-COX).

DMD Fast Forward. Published on February 23, 2022 as DOI: 10.1124/dmd.121.000624
This article has not been copyedited and formatted. The final version may differ from this version.

Supernatants were collected after centrifugation at 16,100 g for 10 min at 4°C for subsequent ultra-high pressure liquid chromatography-mass spectrometry (UHPLC-MS/MS) analysis. Pooled HLM without any inhibitor was used as the reference reaction, and all assays were performed in triplicate.

Enzyme kinetic assays. HEK293 cells individually overexpressing V5-tagged CYPs 1A2, 2A6, 2B6, 2C8, 2C9, 2C19, 2D6, 2E1 and 3A4 were previously described and used in the present kinetic analyses (Peterson et al., 2017a). Microsomal membrane fractions of CYP-overexpressing cell lines were prepared by differential centrifugation as previously described (Dellinger et al., 2006; Peterson et al., 2017b). For the determination of relative CYP quantification for each microsomal preparation, equal amounts of microsomal protein (20 µg) were loaded on 10% SDS-polyacrylamide gels, with CYP protein quantity determined by Western blot analysis using the anti-V5-HRP antibody at a 1:2,500 dilution. As a loading control for microsomal fractions, the anti-calnexin-HRP antibody was used at a 1:5,000 dilution for all Western blots. Image J software was used to perform densitometry analysis (Rasband, 1997), and the relative expression of each CYP-containing microsomal preparation was used for normalization in *N*-oxidation activity assays.

N-oxidation reactions (final volume = 12.5 µL) contained 50 µg of total microsomal protein, 50 mM potassium phosphate, a NADPH regenerating system (1.55 mmol/L NADP+, 3.3 mmol/L glucose-6-phosphate, 3.3 mmol/L $MgCl_2$, 0.5 of 40 U/mL glucose-6-phosphate dehydrogenase) and varying concentrations of COT (0.05 – 1,000 µM). All incubations were performed for 30 min at 37°C, with reactions terminated by

DMD Fast Forward. Published on February 23, 2022 as DOI: 10.1124/dmd.121.000624
This article has not been copyedited and formatted. The final version may differ from this version.

the addition of ice-cold acetonitrile to a final volume of 125 µL. Supernatants were collected after centrifugation at 16,100 g for 10 min at 4°C and 0.001 ppm internal standard (D_3-COX) was added prior to subsequent UHPLC-MS/MS analysis. Pooled commercial HLM and untransfected parent HEK293 cell microsomes (50 µg) were used as the source for positive and negative assay controls, respectively.

UHPLC-MS/MS analysis. UHPLC-MS/MS was performed on a UPLC-BEH-HILIC column (2.1 x 100 mm, 1.7 µm) with a mobile phase that consisted of 5 mmol/L sodium acetate (pH 6.7) in either 50% acetonitrile (v/v) (buffer A) or 90% acetonitrile (buffer B). A gradient elution was used as follows: 20% buffer A for 1.5 min, a linear gradient to 100% buffer A from 1.5-2.5 min, maintenance of 100 % buffer A for 3 min, and a re-equilibrium step to the initial 20% buffer A conditions from 5.5 to 7 min (flow rate 0.4 $mL \cdot min^{-1}$). The injection volume was 5 µL and the column temperature was 30ºC. MS/MS detection was performed in a Waters ACQUITY XEVO TQD instrument in MRM ESI+ mode. An MRM method was performed using the following mass transitions: m/z 177.103→98.0, 193.1→96.0, and 196.1→96.0 to monitor COT, COX, and D_3-COX, respectively. The desolvation temperature was 500°C, with 800 L/h of nitrogen gas. The collision energy was optimized at 27 V, 21 V and 21 V for COT, COX, and D_3-COX, respectively. A cone voltage of 30 V and 0.5 s dwell time resulted in high-sensitivity detection of COX and D_3-COX. Peak retention times observed in the enzymatic incubations were compared with the retention time of the respective D_3 internal standard.

DMD Fast Forward. Published on February 23, 2022 as DOI: 10.1124/dmd.121.000624
This article has not been copyedited and formatted. The final version may differ from this version.

The specificity of all LC-MS/MS methods were validated using positive and negative control samples as well as by comparing peaks with those observed for purchased standards and isotope-labeled internal standards. Linearity was validated by $r^2 > 0.997$ for all standard curves. Since isotope-labeled internal standards were utilized in all LC-MS/MS analysis, matrix effects on analyte quantification was minimal. For quantification of COX and 3HC, HLM assays were directly spiked with COX or 3HC standard (0.001 ppm each) and then analyzed by LC-MS/MS without sample extraction. Therefore, recovery or dilution effects were not a concern. Analyte quantification was based on the ratio of signal peak area vs. the peak area of the internal standard.

Stability studies were performed by quantifying COX levels post-extraction in HLM assays by LC-MS/MS, and then repeating the quantification by LC-MS/MS after incubating the extracted COX after 24 h at 8^{o}C. This was the longest time taken to run any given sample in our LC-MS/MS analysis. The stability of COX varied by no more than 10%.

Assay precision and accuracy was validated by repeated sample quantification on LC-MS/MS. This was performed by preparing 5 individual samples of reaction matrix containing 1 ppm of COX standard, processing them for LC-MS/MS, and immediately measuring COX concentrations for each sample by LC-MS/MS as compared to individually prepared standard curves also measured by LC-MS/MS. The mean recovery for the 5 samples was 88.3% and the coefficient of variation (CV) for these samples was 3.1%, indicating high accuracy and precision for these studies. The lower limit of detection for the experimental system used ranged from 0.049 - 0.98 µM for cotinine, COX, and 3HC, with quantification ranging from 0.049 - 10 µM for cotinine and COX and 0.098 – 10 µM for 3HC (see UHPLC-MS/MS performance parameters in Supp. Table 2).

DMD Fast Forward. Published on February 23, 2022 as DOI: 10.1124/dmd.121.000624
This article has not been copyedited and formatted. The final version may differ from this version.

COT *N*-oxidation assays in HLM. Microsomes from the 113 individual human liver specimens obtained from the H. Lee Moffitt Cancer Center were utilized for these studies. Assays were performed as described above using 25 µg of total microsomal protein and 500 µM of cotinine as substrate. D_3-3HC and D_3-COX (0.001 ppm) was added to the stopped reaction immediately prior to UHPLC-MS/MS analysis. In addition to the detection of COX, D3-COX, and COT, 3HC and D_3-3HC formation was also monitored in the same reaction. The same UHPLC-MS/MS method described above was performed for the present study with the addition of the following MS/MS mass transitions: m/z 193.1→80.0 and 196.1→80.0, to monitor 3HC and D_3-3HC, respectively. The cone voltage and collision energy were optimized at 20 V for both 3HC and D_3-3HC. Metabolite retention times observed in the enzymatic incubations were compared with retention times of their corresponding D_3 internal standard metabolites. Tissue activity assays were performed in triplicate.

Genotyping of CYPs 2A6, 2B6 and 2C19 in human liver specimens. The potential impact of genetic variation in CYPs 2A6, 2B6 and 2C19 on COT-*N*-oxidation activity was examined by genotyping the same 113 liver specimens used for microsomal activity assays described above for allelic variants that have been associated with altered enzyme expression and/or function and that have a minor allele frequency (MAF) of >0.10 in Caucasians [*CYP2A6*: **2*, **9*, and **14*; *CYP2B6*: **2*, **5*, **9*, *Int1*, and *Int2*; and *CYP2C19*: **2* and **17*; (Ahmad et al., 2017; Binnington et al., 2012; Bloom et al., 2019; Bloom, Harari, et al., 2013; Bloom, Martinez, et al., 2013; Desta et

DMD Fast Forward. Published on February 23, 2022 as DOI: 10.1124/dmd.121.000624
This article has not been copyedited and formatted. The final version may differ from this version.

al., 2002; Fernandez-Salguero et al., 1995; Gervot et al., 1999; Hulot et al., 2006; Pianezza et al., 1998; Pitarque et al., 2001; Sim et al., 2006; Wang et al., 2019)]. High-prevalence functional alleles (MAF>0.05) are not observed for CYP3A4 (Eiselt et al., 2001; Zhou et al., 2017). While high-prevalence alleles are observed for CYP2E1, their functional role has not been clearly established (Hu et al., 1997; Zhou et al., 2017). The non-functional CYP2A6*4 and CYP2A6*7 alleles were not analyzed in this group since all liver donors were from Caucasian subjects, who have a low MAF (<0.03) for these alleles (López-Flores et al., 2017). Genomic DNA from the 113 liver specimens was genotyped using TaqMan probes following manufacturer's suggested protocols. Dilutions of 5 ng DNA/µL were used to perform all genotyping analysis. The following alleles were examined in the liver specimens using Taqman probes: CYP2A6 [*2 (rs1801272; C__27861808), *9 (rs28399433; C__30634332_10) and *14 (rs rs28399435; C__30634234_10)], CYP2B6 [*2 (rs8192709; C__2818162_20), *5 (rs3211371; C__30634242_40), *9 (rs3745274; C__7817765_60), Int1 (rs4803419; C__7817764_10) and Int 2 (rs8109525; C__2818157_10)], and CYP2C19 [*2 (rs4244285; C__25986767_70) and *17 (rs12248560; C__4625986767_70)]. All genotyping reactions were performed in quadruplicate. As the CYP2B6 intron variants 1 and 2 (Int 1 and Int 2) exhibited high linkage disequilibrium in this population (R^2= 0.773), they were considered as a single variant (termed 'Int') for CYP2B6 genotyping analysis.

Statistical analyses. Kinetic parameters were determined from the Michaelis–Menten equation using GraphPad Prism version 6.01 (GraphPad Software, San Diego,

DMD Fast Forward. Published on February 23, 2022 as DOI: 10.1124/dmd.121.000624
This article has not been copyedited and formatted. The final version may differ from this version.

CA). Relative maximum reaction rates (V_{max}) were calculated as pmol COX· L^{-1}·min^{-1}·mg microsomal $protein^{-1}$, with values normalized to the relative expression of each CYP450-overexpressed HEK293 cell microsomal protein preparation as determined by Western blot analysis using the anti-V5 antibody and Image J software as described above.

All reported values represent the results [e.g., mean ± standard deviation (SD)] of three independent experiments. The inhibition of each CYP450 enzyme in HLM was compared to the reaction without any specific inhibitor using a two-tailed Student's t-test. One-way ANOVA followed by a Kruskal-Wallis H test was used to analyze different metabolism phenotype groups within the panel of liver specimens; p-values from ANOVA are reported unless indicated otherwise. A P-value of less than 0.05 was considered the threshold for statistical significance.

DMD Fast Forward. Published on February 23, 2022 as DOI: 10.1124/dmd.121.000624
This article has not been copyedited and formatted. The final version may differ from this version.

Results

Inhibition assays of COX formation in HLM. The effects of enzyme-specific CYP inhibitors in HLM-mediated conversion of COT to COX was examined using UHPLC-MS/MS. As shown in Figure 2 (panel A), a COX peak was observed at a retention time of 1.80 min (middle panel) while the COT substrate peak was observed at 1.06 min (top panel). The retention times of the COX peak were identical to that of D_3-labeled COX standard (bottom panel). In incubations using 10 µM specific inhibitors for CYP enzymes 2B6, 2E1 and 3A4, significant decreases in COX formation of 21% (p =0.033), 16% (p= 0.026), and 33% (p=0.013), respectively, were observed as compared to control assays without inhibitor; no significant inhibition was observed when using these inhibitors at 1 µM (Figure 2, panel B). When tranylcypromine was used to inhibit both CYP2A6 and CYP2C19 in HLM, significant decreases in COX formation of 15% (p= 0.004) and 54% (p=0.002) were observed using 1 µM and 10 µM, respectively. No significant decrease in COX formation was observed when using inhibitors for CYPs 1A2, 2C8, 2C9 and 2D6 at both 1 µM and 10 µM.

Kinetic analysis of COT-*N*-oxide formation. The CYP enzymes that showed significant inhibition for COX formation in HLM when using enzyme-specific inhibitors (CYPs 2A6, 2B6, 2C19, 2E1 and 3A4) were further analyzed for kinetic parameters of COX formation using microsomes from HEK293 cells overexpressing V5-tagged CYP enzymes (Peterson et al., 2017a) with the relative V_{max} values of COX formation calculated based on the relative expression of each CYP enzyme, measured by

DMD Fast Forward. Published on February 23, 2022 as DOI: 10.1124/dmd.121.000624
This article has not been copyedited and formatted. The final version may differ from this version.

densitometry analysis of the V5 antibody signal in Western blots. (Supp. Figure 1). The chosen incubation times and protein concentrations were within the linear range of COT-*N*-oxidation velocity curves for each CYP enzyme tested (data not shown). Representative kinetic plots for COX formation in microsomes from CYP-overexpressing cell lines and in HLM are shown in Figure 3. The highest COX formation activities were observed for microsomes from the CYP2A6- and CYP2C19-overexpressing cell lines (V_{max}/K_M = 44 and 42 nL•min-1•mg-1, respectively; Table 1). CYPs 2A6 and 2C19 also exhibited similar K_M values of 390 µM and 405 µM, respectively; CYP2B6 exhibited a somewhat higher K_M of 810 µM. The average K_M values observed for these three enzymes for COX formation was very similar to the K_M observed for HLM (K_M = 550 µM). In contrast, low affinities for COX formation were observed for CYPs 2E1 and 3A4, with K_M values >10 mM.

COX formation vs CYP genotypes in human liver specimens. *In vitro* COX formation was measured in a panel of 113 HLM by LC-MS/MS as described in the Materials and Methods. The mean rate of COX formation observed for these specimens was 11.8 ± 6.4 pmol•min^{-1}•mg microsomal protein^{-1}, ranging from 0.71 to 31.2 pmol•min^{-1}•mg microsomal protein^{-1} (Table 2). As a measure of CYP2A6 activity, levels of 3HC formation were also quantified in the same specimens. The mean rate of 3HC formation in the same HLM specimens was 28.1 ± 14.9 pmol•min^{-1}•mg microsomal protein^{-1} of 3HC with a range of 3.4 to 101 pmol•min^{-1}•mg microsomal protein^{-1}.

Informative genotyping data was obtained for 113, 109 and 102 subjects tested for polymorphisms in *CYP2C19, CYP2A6* and CYP2B6, respectively, with informative

DMD Fast Forward. Published on February 23, 2022 as DOI: 10.1124/dmd.121.000624
This article has not been copyedited and formatted. The final version may differ from this version.

genotypes obtained for each of the 113 subjects for all CYP2C19 SNPs examined, each of the 109 subjects for all CYP2A6 SNPs examined, and each of the 102 subjects for all CYP2B6 SNPs examined. The MAF observed for each allele in the genotyped specimens is similar to that reported for the CEU population in the 1000 Genomes Project (Supp. Table 3) (*1000 Genomes. Gene: CYP2A6 (ENSG00000255974) - Summary - Homo Sapiens - Ensembl Genome Browser 99*, 2020).

The impact of CYP2C19 variants on COX formation was assessed with *CYP2C19* genotype categorized according to the recommendations of the Clinical Pharmacogenetics Implementation Consortium (CPIC®) (Scott et al., 2013), with ultra-rapid metabolizers (UM_{2C19}) containing the (*17/*17) and (*17/*1) genotypes; extensive metabolizers (EM_{2C19}) consisting of the (*1/*1) 'wild-type' genotype; intermediate metabolizers (IM_{2C19}) containing the (*2/*17) or (*2/*1) genotypes; and poor metabolizers (PM_{2C19}) consisting of the (*2/*2) genotype. The rate (mean ± SD, expressed as pmol•min^{-1}•mg^{-1} microsomal protein) of COX formation in the different metabolizing groups were as follows: UM_{2C19} (12.6 $\pm$ 5.3; n=26), EM_{2C19} (11.9 $\pm$ 6.5; n=62), IM_{2C19} (10.7 $\pm$ 5.4; n=21) and PM_{2C19} (8.4 $\pm$ 4.0; n=4; Figure 4, panel A). While the decreases observed in the different CYP2C19 metabolizing groups were not significant (p_{trend}=0.26), the difference approached significance (p=0.089) when comparing the combined UM_{2C19} + EM_{2C19} groups (11.9 $\pm$ 6.4 pmol•min^{-1}•mg^{-1} microsomal protein) vs the combined IM_{2C19} + PM_{2C19} groups (10.1 $\pm$ 5.3 pmol•min^{-1}•mg^{-1} microsomal protein; Figure 4, panel B). To normalize the specimens based on differences in sample quality and overall enzymatic activity, the COX/3HC ratio was also used as a phenotypic measure. A significant (Kruskal-Wallis test p=0.026) trend towards

DMD Fast Forward. Published on February 23, 2022 as DOI: 10.1124/dmd.121.000624
This article has not been copyedited and formatted. The final version may differ from this version.

decreased mean COX/3HC ratio was observed when comparing the UM_{2C19} (0.55 ± 0.11), EM_{2C19} (0.44 ± 0.19), IM_{2C19} (0.36 ± 0.12), and PM_{2C19} (0.32 ± 0.050) groups (Figure 4, panel C). Significant differences in COX/3HC ratio were also observed when comparing the UM_{2C19} group with the IM_{2C19} (p= 0.0032) and PM_{2C19} (p=0.0058) groups, respectively (Figure 4, panel C). Furthermore, a significant difference in COX/3HC was observed when comparing the combined UM_{2C19} + EM_{2C19} groups vs. the combined IM_{2C19} + PM_{2C19} groups (p=0.017; Figure 4, panel D). While not statistically significant, similar trends were observed for CYP2C19 genotype groups when the analysis was performed only for subjects in the CYP2A6 EM group (n=89, described below; p=0.086; Supp. Figure 2, panel A) or only in the CYP2B6 EM group (n=44, described below; p=0.33; Supp. Figure 2; panel B).

To minimize *CYP2C19* genotype-mediated effects, the effect of *CYP2A6* genotype was analyzed using specimens that were categorized as EM for CYP2C19 (n=62). *CYP2A6* genotype was categorized according to previously reported EM and IM CYP2A6 groups as follows: the EM_{2A6} group included specimens exhibiting the (*1/*1), (*1/*2), (*1/*9) or (*1/*14) genotypes, while the IM_{2A6} group included the (*2/*2), (*9/*9), (*2/*9), (*2/*14), and (*9/*14) genotypes [no subjects were (*14/*14)] (Benowitz et al., 2006). Slow metabolizers for CYP2A6 were not screened in this study since the low-prevalence *4 or *7 alleles were not examined in this population. No significant differences (p=0.70) in the rate (mean ± SD expressed as pmol•min^{-1}•mg microsomal $protein^{-1}$) of COX formation were observed between the EM_{2A6} (12.2 ± 6.6) and IM_{2A6} groups (10.6 ± 6.4; Supp. Figure 2, panel C).

DMD Fast Forward. Published on February 23, 2022 as DOI: 10.1124/dmd.121.000624
This article has not been copyedited and formatted. The final version may differ from this version.

Using specimens that exhibited only EM genotypes for both CYP2C19 and CYP2A6 (n=50), CYP2B6 genotype groups were stratified as follows: the EM_{2B6} group included specimens that exhibited the (*1/*1), (*1/*2) or (*1/*5) genotypes; the IM_{2B6} group included HLM exhibiting the (*1/*9), (*1/Int), (*2/*2), (*2/*5), (*2/*9), (*2/Int), (*5/*5), (*5/*9) or (*5/Int) genotypes; and the PM_{2B6} group included specimens with the (*9/*9), (*9/Int) or (Int/Int) genotypes. No significant differences in the rate (mean ± SD expressed as pmol•min^{-1}•mg^{-1} microsomal protein) of COX formation were observed in the different CYP2B6 metabolism phenotype groups [EM_{2B6} (12.48 $\pm$ 5.32) vs. IM_{2B6} (10.13 $\pm$ 6.28) vs. PM_{2B6} (9.45 $\pm$ 7.41); p=0.14; results not shown]. The COX/3HC ratios of 0.46 (n=7) for the EM_{2B6} group, 0.50 (n=20) for the IM_{2B6} group and 0.40 (n=23) for the PM_{2B6} group were also not significantly different (p= 0.51 Supp. Figure 2, panel D). In addition, no significant differences in COX formation or COX/3HC ratio were observed when comparing the PM_{2B6} vs EM_{2B6} + IM_{2B6} groups (results not shown).

DMD Fast Forward. Published on February 23, 2022 as DOI: 10.1124/dmd.121.000624
This article has not been copyedited and formatted. The final version may differ from this version.

Discussion

The involvement of CYP2A6 in the formation of COT from nicotine and 3HC from COT is well-established (Miki et al., 1996). Studies examining the enzymology of cotinine metabolite formation have also been previously performed for COT-glucuronide and norcotinine (Brown et al., 2005; G. Chen et al., 2007). The present study is the first to examine the major hepatic enzymes important in the formation of COX, which accounts for up to 9% of total cotinine metabolites in the urine of smokers (Rangiah et al., 2011) This pathway may be particularly important for COT excretion in individuals with functionally-deficient CYP2A6 and/or UGT2B10 genotypes where urinary COT levels may be altered, an effect similar to that observed for nicotine-*N'*-oxide formation in subjects with altered CYP2A6 activities (Perez-Paramo et al., 2019; Yamanaka et al., 2004). In the present studies, experiments using HLM demonstrated that up to 54% of COX formation was inhibited using tranylcypromine, an inhibitor of both CYP2A6 and CYP2C19, while COX formation decreased by 21% in HLM using clopidogrel, a specific inhibitor of CYP2B6. Up to 33% of COX formation was inhibited using ketoconazole an inhibitor of CYP3A4, suggesting that this enzyme may also play an important role in COX formation. However, while microsomes from CYP3A4-overexpressing cells exhibited a high Vmax [a pattern similar to that observed previously for this enzyme for other substrates (Sevrioukova & Poulos, 2013)], the substrate affinity of this enzyme for COT was low. It is possible that CYP3A4 may play more of a role in COX formation when cotinine levels are very high within a smoker. Other than CYP2E1, which showed low substrate affinity in CYP2E1 over-expressing cell microsomes and marginal activity

DMD Fast Forward. Published on February 23, 2022 as DOI: 10.1124/dmd.121.000624
This article has not been copyedited and formatted. The final version may differ from this version.

in inhibition studies, no other hepatic CYP enzyme screened in this study (CYPs 1A2, 2C8, 2C9 and 2D6) exhibited detectable COX formation activity. Kinetic analysis using microsomes from CYP-overexpressing cell lines demonstrated similar K_M values for CYP2A6 (390 μM) and CYP2C19 (405 μM) for COX formation; a nearly 2-fold higher K_M was observed for microsomes from CYP2B6-overexpressing cells (810 μM). The K_M values of these three CYP enzymes were similar to that observed for pooled HLM (K_M = 550 μM), suggesting that potentially all three of these CYP enzymes could contribute to COX formation in smokers.

This is the first study demonstrating the importance of CYP2C19 in nicotine metabolism. The intrinsic clearance of COX formation by microsomes from CYP2C19-overexpressing cells in the present study was very similar to that observed for CYP2A6 (4.2 vs 4.4 $nL \cdot mL^{-1} \cdot$mg microsomal $protein^{-1}$, normalized to CYP enzyme expression as determined by Western blotting). Previous studies suggest that CYP2C19 protein expression is at least three times that of CYP2A6 in human liver (Achour et al., 2014; Shimada et al., 1994), suggesting that CYP2C19 may play a more important role than CYP2A6 in COX formation.

CYP2B6 has been previously reported to be involved in nicotine metabolism including in the formation of COT from nicotine, where it exhibits a K_M (550 μM) (Yamanaka et al., 2005) approximately 5.8 times higher than that observed for CYP2A6 (95 μM) (Yamanaka et al., 2005). CYP2B6 was also suggested to be involved in the formation of (S)-nornicotine-iminium and (S)-nornicotine, with K_M values ranging from 184 to 269 μM (Bloom et al., 2019). This contrasts with the higher K_M observed for CYP2B6 for COX formation (810 μM). CYP2B6 was shown in previous studies to exhibit

DMD Fast Forward. Published on February 23, 2022 as DOI: 10.1124/dmd.121.000624
This article has not been copyedited and formatted. The final version may differ from this version.

lower levels of hepatic expression than CYP2C19 and to be expressed at levels similar to that observed for CYP2A6 (Achour et al., 2014; Shimada et al., 1994). Together, these data suggest that, of the three enzymes, CYP2B6 may be playing a more minor role in COX formation.

Most interestingly, COX formation in HLM were significantly associated with CYP2C19 genotypes in the present study. CYP2C19 variants significantly modified COX formation by up to 35% when comparing the UM_{2C19} group and PM_{2C19} groups, and 25% when comparing the UM_{2C19} and IM_{2C19} groups. These results are consistent with that observed previously for CYP2C19 genotypes on drug metabolism, including agents like clopidogrel, omeprazole, voriconazole, which show increased enzyme efficacy by up to 35-40% in the UM_{2C19}/EM_{2C19} genotype groups when compared to the PM_{2C19} genotype group (Li-Wan-Po et al., 2010).

While CYP2A6 showed similar activity as CYP2C19 in the kinetics analysis, CYP2A6 genetic variants were not significantly associated with an altered COX formation phenotype. This pattern is consistent with the lower level of expression of CYP2A6 as compared to CYP2C19 in human liver (Achour et al., 2014; Shimada et al., 1994). However, since CYP2A6 is the enzyme responsible for 3HC conversion (Miki et al., 1996), the COX/3HC ratio could not be used in this case to correct for differences in enzyme quality between specimens. Additionally, CYP2A6 alleles that would correspond with poor metabolizer subjects (carriers of the CYP2A6 *4 or *7 alleles) were not included in this study due to low allelic frequency in the studied population.

No differences in the levels of observed COX formation or as COX expressed as a ratio with 3HC were observed for CYP2B6 genotypes in the present study. Previous

DMD Fast Forward. Published on February 23, 2022 as DOI: 10.1124/dmd.121.000624
This article has not been copyedited and formatted. The final version may differ from this version.

studies have suggested that CYP2B6 may be more important in nicotine metabolism when CYP2A6 function is impaired (Al Koudsi & Tyndale, 2010; Dicke et al., 2005). Additionally, an effect by variant CYP2B6 genotypes on COX formation could not be adequately tested in subjects with CYP2A6-deficient genotypes given the small sample number of specimens from subjects who were IM_{2A6} (n=5) and the fact that poor metabolizers of CYP2A6 were not assessed in this population. Further analysis of a large sample size of intermediate and poor CYP2A6 metabolizer subjects will be required to better determine the extent of the influence of CYP2B6 as well as CYP2A6 on COX formation.

In summary, this is the first study to report on the major hepatic enzymes important in COX formation, with CYP2C19 playing an important role. This study also demonstrates CYP2C19-mediated genetic effects on COX formation in a panel of human liver specimens, an effect that could potentially modify the NMR in smokers and could affect pharmacotherapeutic decisions for smoking cessation treatment. Further population-based studies involving genotype-phenotype associations should be performed to better assess the effect of CYP2C19 on COX formation and the NMR.

DMD Fast Forward. Published on February 23, 2022 as DOI: 10.1124/dmd.121.000624
This article has not been copyedited and formatted. The final version may differ from this version.

Acknowledgements

The authors thank Dr. Senthil Natesan in the Department of Pharmaceutical Sciences at the Washington State University College of Pharmacy and Pharmaceutical Sciences for his helpful suggestions and discussion. The authors also thank the Mass Spectrometry Core facility at Washington State University Spokane for their help with LC/MS.

DMD Fast Forward. Published on February 23, 2022 as DOI: 10.1124/dmd.121.000624
This article has not been copyedited and formatted. The final version may differ from this version.

Authorship Contributions

Participated in research design: Perez-Paramo, Watson, Chen, Lazarus.

Conducted experiments: Perez-Paramo.

Contributed new reagents or analytic tools: NA.

Performed data analysis: Perez-Paramo, Watson, Chen, Lazarus.

Wrote or contributed to the writing of the manuscript: Perez-Paramo, Watson, Lazarus.

DMD Fast Forward. Published on February 23, 2022 as DOI: 10.1124/dmd.121.000624
This article has not been copyedited and formatted. The final version may differ from this version.

References

1000 genomes. Gene: CYP2A6 (ENSG00000255974) - Summary - Homo sapiens - Ensembl genome browser 99. (2020). Ensembl GRCh37 Release 9. http://uswest.ensembl.org/Homo_sapiens/Gene/Summary?db=core;g=ENSG00000255974;r=19:40843541-40850447

Achour, B., Barber, J., & Rostami-Hodjegan, A. (2014). Expression of hepatic drug-metabolizing cytochrome P450 enzymes and their intercorrelations: A meta-analysis. *Drug Metabolism and Disposition*, *42*(8), 1349–1356. https://doi.org/10.1124/dmd.114.058834

Ahmad, T., Sabet, S., Primerano, D. A., Richards-Waugh, L. L., & Rankin, G. O. (2017). Tell-Tale SNPs: The Role of CYP2B6 in Methadone Fatalities. *Journal of Analytical Toxicology*, *41*(4), 325–333. https://doi.org/10.1093/JAT/BKW135

Al Koudsi, N., & Tyndale, R. F. (2010). Hepatic CYP2B6 is altered by genetic, physiologic, and environmental factors but plays little role in nicotine metabolism. *Xenobiotica*, *40*(6), 381–392. https://doi.org/10.3109/00498251003713958

Baurley, J. W., Edlund, C. K., Pardamean, C. I., Conti, D. V., Krasnow, R., Javitz, H. S., Hops, H., Swan, G. E., Benowitz, N. L., & Bergen, A. W. (2016). Genome-wide association of the laboratory- based nicotine metabolite ratio in three ancestries. *Nicotine and Tobacco Research*, *18*(9), 1837–1844. https://doi.org/10.1093/ntr/ntw117

Benowitz, N. L., Swan, G. E., Jacob, P., Lessov-Schlaggar, C. N., & Tyndale, R. F. (2006). CYP2A6 genotype and the metabolism and disposition kinetics of nicotine. *Clinical Pharmacology and Therapeutics*, *80*(5), 457–467. https://doi.org/10.1016/j.clpt.2006.08.011

Berg, J. Z., Von Weymarn, L. B., Thompson, E. A., Wickham, K. M., Weisensel, N. A., Hatsukami, D. K., & Murphy, S. E. (2010). UGT2B10 genotype influences nicotine glucuronidation, oxidation, and consumption. *Cancer Epidemiology Biomarkers and Prevention*, *19*(6), 1423–1431. https://doi.org/10.1158/1055-9965.EPI-09-0959

Binnington, M. J., Zhu, A. Z. X., Renner, C. C., Lanier, A. P., Hatsukami, D. K., Benowitz, N. L., & Tyndale, R. F. (2012). CYP2A6 and CYP2B6 genetic variation and its association with nicotine metabolism in South Western Alaska Native people. *Pharmacogenet Genomics*, *22*(6), 429–440. https://doi.org/10.1097/FPC.0b013e3283527c1c.CYP2A6

Bloom, A. J., Harari, O., Martinez, M., Zhang, X., McDonald, S. A., Murphy, S. E., & Goate, A. (2013). A compensatory effect upon splicing results in normal function of the CYP2A6*14 allele. *Pharmacogenetics and Genomics*, *23*(3), 107–116. https://doi.org/10.1016/j.biotechadv.2011.08.021.Secreted

Bloom, A. J., Martinez, M., Chen, L. S., Bierut, L. J., Murphy, S. E., & Goate, A. (2013). CYP2B6 non-coding variation associated with smoking cessation is also associated with differences in allelic expression, splicing, and nicotine metabolism independent of common amino-acid changes. *PLoS ONE*, *8*(11), 1–13. https://doi.org/10.1371/journal.pone.0079700

Bloom, A. J., Wang, P. F., & Kharasch, E. D. (2019). Nicotine oxidation by genetic variants of CYP2B6 and in human brain microsomes. *Pharmacology Research and*

Perspectives, *7*(2), 1–8. https://doi.org/10.1002/prp2.468

Brown, K. M., Von Weymarn, L. B., & Murphy, S. E. (2005). Identification of N-(hydroxymethyl) norcotinine as a major product of cytochrome P450 2A6, but not cytochrome P450 2A13-catalyzed cotinine metabolism. *Chemical Research in Toxicology*, *18*(12), 1792–1798. https://doi.org/10.1021/tx0501381

Chen, G., Blevins-Primeau, A. S., Dellinger, R. W., Chen, G., Blevins-primeau, A. S., Dellinger, R. W., Muscat, J. E., & Lazarus, P. (2007). Glucuronidation of Nicotine and Cotinine by UGT2B10 : Loss of Function by the UGT2B10 Codon 67 (Asp > Tyr) Polymorphism Function by the UGT2B10 Codon 67 (Asp > Tyr) Polymorphism. *Cancer Research*, *67*(19), 9024–9029. https://doi.org/10.1158/0008-5472.CAN-07-2245

Chen, G., Giambrone, N. E., & Lazarus, P. (2012). Glucuronidation of trans-3'-hydroxycotinine by UGT2B17 and UGT2B10. *Pharmacogenetics and Genomics*, *22*(3), 183–190. https://doi.org/10.1097/FPC.0b013e32834ff3a5

Chen, G., Giambrone NE Jr, Dluzen, D. F., Muscat, J. E., Berg, A., Gallagher, C. J., & Lazarus, P. (2010). Glucuronidation genotypes and nicotine metabolic phenotypes: Importance of UGT2B10 and UGT2B17 knock-out polymorphisms. *Cancer Research*, *70*(19), 7543–7552. https://doi.org/10.1158/0008-5472.CAN-09-4582.Glucuronidation

Chen, L.-S., Horton, A., & Bierut, L. (2018). Pathways to precision medicine in smoking cessation treatments. *Neuroscience Letters*, *669*, 83–92. https://doi.org/10.1016/j.neulet.2016.05.033

Chenoweth, M. J., Novalen, M., Jr, L. W. H., Schnoll, R. A., George, T. P., Cinciripini, P. M., Lerman, C., & Tyndale, R. F. (2014). Known and Novel Sources of Variability in the Nicotine Metabolite Ratio in a Large Sample of Treatment-Seeking Smokers. *Cancer Epidemiol Biomarkers Prev*, *23*(9), 1773–1782. https://doi.org/10.1158/1055-9965.EPI-14-0427

Coughtrie, M. W. H., Burchell, B., & Bend, J. R. (1987). Purification and properties of rat kidney UDP-glucuronosyltransferase. *Biochemical Pharmacology*, *36*(2), 245–251. https://doi.org/10.1016/0006-2952(87)90696-4

Dagne, E., & Castagnoli, N. (1972). Cotinine N-Oxide, a New Metabolite of Nicotine. *Journal of Medicinal Chemistry*, *15*(8), 840–841. https://doi.org/10.1021/jm00278a011

Dellinger, R. W., Fang, J. L., Chen, G., Weinberg, R., & Lazarus, P. (2006). Importance of UDP-glucuronosyltransferase 1A10 (UGT1A10) in the detoxification of polycyclic aromatic hydrocarbons: Decreased glucuronidative activity of the UGT1A10139LYS isoform. *Drug Metabolism and Disposition*, *34*(6), 943–949. https://doi.org/10.1124/dmd.105.009100

Dempsey, D., Tutka, P., Iii, P. J., Allen, F., Tyndale, R. F., Benowitz, N. L., & Francisco, S. (2004). Nicotine metabolite ratio as an index of cytochrome P450 2A6 metabolic activity. *Clinical Pharmacology & Therapeutics*, *450*, 64–72. https://doi.org/10.1016/j.clpt.2004.02.011

Desta, Z., Zhao, X., Shin, J. G., & Flockhart, D. A. (2002). Clinical significance of the cytochrome P450 2C19 genetic polymorphism. *Clinical Pharmacokinetics*, *41*(12), 913–958. https://doi.org/10.2165/00003088-200241120-00002

Dicke, K. E., Skrlin, S. M., & Murphy, S. E. (2005). Nicotine and 4-(methylnitosamino)-1-

(3-pyridyl)-butanone metabolism by cytochrome P450 2B6. *Drug Metabolism and Disposition*, *33*(12), 1760–1764. https://doi.org/10.1124/dmd.105.006718.nornicotine

Draper, A. J., Madan, A., & Parkinson, A. (1997). Inhibition of coumarin 7-hydroxylase activity in human liver microsomes. *Archives of Biochemistry and Biophysics*, *341*(1), 47–61. https://doi.org/10.1006/abbi.1997.9964

Eiselt, R., Domanski, T. L., Zibat, A., Mueller, R., Presecan-Siedel, E., Hustert, E., Zanger, U. M., Brockmoller, J., Klenk, H. P., Meyer, U. A., Khan, K. K., He, Y. A., Halpert, J. R., & Wojnowski, L. (2001). Identification and functional characterization of eight CYP3A4 protein variants. *Pharmacogenetics*, *11*(5), 447–458. https://doi.org/10.1097/00008571-200107000-00008

Falcone, M., Jepson, C., Ph, D., Benowitz, N., Bergen, A. W., Ph, D., Lerman, C., Ph, D., Ray, R., & Ph, D. (2011). *Association of the Nicotine Metabolite Polymorphisms With Smoking Rate Among Treatment-Seeking Smokers*. *13*(6), 498–503. https://doi.org/10.1093/ntr/ntr012

Fernandez-Salguero, P., Hoffman, S. M. G., Cholerton, S., Mohrenweiser, H., Raunio, H., Rautio, A., Pelkonen, O., Huang, J. D., Evans, W. E., Idle, J. R., & Gonzalez, F. J. (1995). A genetic polymorphism in coumarin 7-hydroxylation: Sequence of the human CYP2A genes and identification of variant CYP2A6 alleles. *American Journal of Human Genetics*, *57*(3), 651–660.

Fix, B. V, O'Connor, R. J., Benowitz, N., Heckman, B. W., Cummings, K. M., Fong, G. T., & Thrasher, J. F. (2017). Nicotine Metabolite Ratio (NMR) Prospectively Predicts Smoking Relapse: Longitudinal Findings From ITC Surveys in Five Countries. *Nicotine & Tobacco Research*, *19*(9), 1040–1047. https://doi.org/10.1093/ntr/ntx083

Foth, H., Aubrecht, J., Hohne, M., Walther, U. I., & Kahl, G. F. (1992). Increased cotinine elimination and cotinine-N-oxide formation by phenobarbital induction in rat and mouse. *The Clinical Investigator*, *70*, 175–181.

Gervot, L., Rochat, B., Gautier, J. C., Bohnenstengel, F., Kroemer, H., de Berardinis, V., Martin, H., Beaune, P., & de Waziers, I. (1999). Human CYP2B6: expression, inducibility and catalytic activities. *Pharmacogenetics*, *9*(3), 295–306.

Gorrod, J. W., & Peyton, J. I. (1999). Analytical Determination of Nicotine and Related Compounds and their Metabolites. In *Analytical Determination of Nicotine and Related Compounds and their Metabolites*. Elsevier. https://doi.org/10.1016/b978-0-444-50095-3.x5000-1

Hu, Y., Oscarson, M., Johansson, I., Yue, Q. Y., Dahl, M. L., Tabone, M., Arincò, S., Albano, E., & Ingelman-Sundberg, M. (1997). Genetic polymorphism of human CYP2E1: characterization of two variant alleles. *Molecular Pharmacology*, *51*(3), 370–376.

Hukkanen, J., Jacob, P., & Benowitz, N. L. (2005). Metabolism and disposition kinetics of nicotine. *Pharmacological Reviews*, *57*(1), 79–115. https://doi.org/10.1124/pr.57.1.3

Hulot, J. S., Bura, A., Villard, E., Azizi, M., Remones, V., Goyenvalle, C., Aiach, M., Lechat, P., & Gaussem, P. (2006). Cytochrome P450 2C19 loss-of-function polymorphism is a major determinant of clopidogrel responsiveness in healthy subjects. *Blood*, *108*(7), 2244–2247. https://doi.org/10.1182/blood-2006-04-013052

Jacobson, G. A., & Ferguson, S. G. (2014). Relationship between cotinine and trans-3′-hydroxycotinine glucuronidation and the nicotine metabolite ratio in Caucasian smokers. *Biomarkers*, *19*(8), 679–683. https://doi.org/10.3109/1354750X.2014.966254

Jarvis, M. J., Russell, M. A. H., Benowitz, N. L., & Feyerabend, C. (1988). Elimination of cotinine from body fluids: Implications for noninvasive measurement of tobacco smoke exposure. *American Journal of Public Health*, *78*(6), 696–698. https://doi.org/10.2105/AJPH.78.6.696

Jenner, P., Gorrod, J. W., & Beckett, A. H. (1971). Comparative c- and n-oxidation of (+ and (-)-nicotine by various species. *Xenobiotica*, *1*(4–5), 497–498. https://doi.org/10.3109/00498257109041515

Lerman, C., Schnoll, R. A., Hawk, L. W., Cinciripini, P., George, T. P., Wileyto, E. P., Swan, G. E., Benowitz, N. L., Heitjan, D. F., & Tyndale, R. F. (2015). Use of the nicotine metabolite ratio as a genetically informed biomarker of response to nicotine patch or varenicline for smoking cessation: A randomised, double-blind placebo-controlled trial. *Lancet Respir Med*, *3*(2), 131–138. https://doi.org/10.1016/S2213-2600(14)70294-2

Lerman, C., Tyndale, R., Patterson, F., Wileyto, E. P., Shields, P. G., & Pinto, A. (2006). Nicotine metabolite ratio predicts efficacy of transdermal nicotine for smoking cessation. *Clinical Pharmacology & Therapeutics*, *79*(6), 600–608. https://doi.org/10.1016/j.clpt.2006.02.006

Li-Wan-Po, A., Girard, T., Farndon, P., Cooley, C., & Lithgow, J. (2010). Pharmacogenetics of CYP2C19 : functional and clinical implications of a new variant CYP2C19 * 17. *British Journal of Clinical Pharmacology*, *69*(3), 222–230. https://doi.org/10.1111/j.1365-2125.2009.03578.x

López-Flores, L. A., Pérez-Rubio, G., & Falfán-Valencia, R. (2017). Distribution of polymorphic variants of CYP2A6 and their involvement in nicotine addiction. *EXCLI Journal*, *16*, 174–196. https://doi.org/10.17179/excli2016-847

Malaiyandi, V., Lerman, C., Benowitz, N. L., Jepson, C., Patterson, F., & Tyndale, R. F. (2006). Impact of CYP2A6 genotype on pretreatment smoking behaviour and nicotine levels from and usage of nicotine replacement therapy. *Molecular Psychiatry*, *11*(4), 400–409. https://doi.org/10.1038/sj.mp.4001794

Marclay, F., Grata, E., Perrenoud, L., & Saugy, M. (2011). A one-year monitoring of nicotine use in sport: Frontier between potential performance enhancement and addiction issues. *Forensic Science International*, *213*(1–3), 73–84. https://doi.org/10.1016/j.forsciint.2011.05.026

Maurice, M., Pichard, L., Daujat, M., Fabre, I., Joyeux, H., Domergue, J., & Maurel, P. (1992). Effects of imidazole derivatives on cytochromes P450 from human hepatocytes in primary culture. *FASEB Journal*, *6*(2), 752–758. https://doi.org/10.1096/FASEBJ.6.2.1371482

Miki Nakajima, Toshinori Yamamoto, Ken-Ichi Nunoya, Tsuyoshi Yokoi, Kazuo Nagashima, Kazuaki Inoue, Yoshihiko Funae, Noriaki Shimada, T. K. and Y. K. (1996). Characterization of CYP2A6 Involved in 3'-Hydroxylation of Cotinine in human Liver microsomes. *Pharmacology and Experimental Therapeutics*, *277*(2), 1010–1015.

Miners, J. O., Smith, K. J., Robson, R. A., McManus, M. E., Veronese, M. E., & Birkett,

D. J. (1988). Tolbutamide hydroxylation by human liver microsomes. Kinetic characterisation and relationship to other cytochrome P-450 dependent xenobiotic oxidations. *Biochemical Pharmacology*, *37*(6), 1137–1144. https://doi.org/10.1016/0006-2952(88)90522-9

Murphy, S. E. (2017). Nicotine Metabolism and Smoking: Ethnic Differences in the Role of P450 2A6. *Chem. Res. Toxicol*, *30*, 410–419. https://doi.org/10.1021/acs.chemrestox.6b00387

Murphy, S. E., Park, S. S. L., Thompson, E. F., Wilkens, L. R., Patel, Y., Stram, D. O., & Le Marchand, L. (2014). Nicotine N-glucuronidation relative to N-oxidation and C-oxidation and UGT2B10 genotype in five ethnic/racial groups. *Carcinogenesis*, *35*(11), 2526–2533. https://doi.org/10.1093/carcin/bgu191

Murphy, S. E., Sipe, C. J., Choi, K., Raddatz, L. M., Koopmeiners, J. S., Donny, E. C., & Hatsukami, D. K. (2017). Low cotinine glucuronidation results in higher serum and saliva cotinine in African American compared to White smokers. *Cancer Epidemiol Biomarkers Prev*, *26*(7), 1093–1099. https://doi.org/10.1158/1055-9965.EPI-16-0920

Nakajima, M., Toshinori, Y., Nunoya, K., Yokoi, T., Nagashima, K., Inoue, K., Funae, Y., Shimada, T., Kamataki, T., & Kuroiwa, Y. (1996). Role of human cytochrome P4502A6 in C-oxidation of nicotine. *Drug Metabolism and Disposition*, *24*(11), 1212–1217.

Pellegrini, M., Marchei, L., Rossi, S., Vagnarelli, F., Durgbanshi, A., García-Algar, O., Vall, O., & Pichini, S. (2007). Liquid chromatography/electrospray ionization tandem mass spectrometry assay for determination of nicotine and metabolites, caffeine and arecoline in breast milk. *Rapid Communications in Mass Spectrometry : RCM*, *21*(16), 2693–2703. https://doi.org/10.1002/RCM.3137

Perez-Paramo, Y. X., Chen, G., Ashmore, J. H., Watson, C. J. W., Nasrin, S., Adams-Haduch, J., Wang, R., Gao, Y. T., Koh, W. P., Yuan, J. M., & Lazarus, P. (2019). Nicotine-N'-oxidation by flavin monooxygenase enzymes. *Cancer Epidemiology Biomarkers and Prevention*, *28*(2), 311–320. https://doi.org/10.1158/1055-9965.EPI-18-0669

Peterson, A., Xia, Z., Chen, G., & Lazarus, P. (2017a). Exemestane potency is unchanged by common nonsynonymous polymorphisms in CYP19A1: results of a novel anti-aromatase activity assay examining exemestane and its derivatives. *Pharmacology Research & Perspectives*, *5*(3), e00313. https://doi.org/10.1002/prp2.313

Peterson, A., Xia, Z., Chen, G., & Lazarus, P. (2017b). In vitro metabolism of exemestane by hepatic cytochrome P450s: impact of nonsynonymous polymorphisms on formation of the active metabolite 17 *β* -dihydroexemestane. *Pharmacology Research & Perspectives*, *5*(3), e00314. https://doi.org/10.1002/prp2.314

Pianezza, M. L., Sellers, E. M., & Tyndale, R. F. (1998). Nicotine metabolism defect reduces smoking. *Nature*, *393*, 750.

Pitarque, M., Von Richter, O., Oke, B., Berkkan, H., Oscarson, M., & Ingelman-Sundberg, M. (2001). Identification of a single nucleotide polymorphism in the TATA box of the CYP2A6 gene: Impairment of its promoter activity. *Biochemical and Biophysical Research Communications*, *284*, 455–460.

https://doi.org/10.1006/bbrc.2001.4990
Rangiah, K., Hwang, W.-T., Mesaros, C., Vachani, A., & Blair, I. A. (2011). Nicotine exposure and metabolizer phenotypes from ana lysis of urinary nicotine and its 15 metabolites by LC–MS. *Bioanalysis*, *3*(7), 745–761. https://doi.org/10.4155/BIO.11.42
Rasband, W. S. N. institutes of health. (1997). *Image J*. ImageJ, U. S. National Institutes of Health.
Richter, T., Mürdter, T. E., Heinkele, G., Pleiss, J., Tatzel, S., Schwab, M., Eichelbaum, M., & Zanger, U. M. (2004). Potent Mechanism-Based Inhibition of Human CYP2B6 by Clopidogrel and Ticlopidine. *Journal of Pharmacology and Experimental Therapeutics*, *308*(1), 189–197. https://doi.org/10.1124/jpet.103.056127
Scott, S. A., Sangkuhl, K., Stein, C. M., Hulot, J., Mega, J. L., Roden, D. M., Klein, T. E., & Sabatine, M. S. (2013). Clinical Pharmacogenetics Implementation Consortium Guidelines for CYP2C19 Genotype and Clopidogrel Therapy : 2013 Update. *Clinical Pharmacology & Therapeutics*, *94*(3), 317–323. https://doi.org/10.1038/clpt.2013.105
Sesardic, D., Boobis, A., Murray, B., Murray, S., Segura, J., de la Torre, R., & Davies, D. (1990). Furafylline is a potent and selective inhibitor of cytochrome P450IA2 in man. *British Journal of Clinical Pharmacology*, *29*(6), 651–663. https://doi.org/10.1111/j.1365-2125.1990.tb03686.x
Sevrioukova, I. F., & Poulos, T. L. (2013). Understanding the mechanism of cytochrome P450 3A4: Recent advances and remaining problems. *Dalton Transactions*, *42*(9), 3116–3126. https://doi.org/10.1039/c2dt31833d
Shimada, T., Yamazaki, H., Mimura, M., Inui, Y., & Guengerich, F. P. (1994). Interindividual variations in human liver cytochrome P-450 enzymes involved in the oxidation of drugs, carcinogens and toxic chemicals: studies with liver microsomes of 30 Japanese and 30 Caucasians. *The Journal of Pharmacology and Experimental Therapeutics*, *270*(1), 414–423.
Sim, S. C., Risinger, C., Dahl, M. L., Aklillu, E., Christensen, M., Bertilsson, L., & Ingelman-Sundberg, M. (2006). A common novel CYP2C19 gene variant causes ultrarapid drug metabolism relevant for the drug response to proton pump inhibitors and antidepressants. *Clinical Pharmacology and Therapeutics*, *79*(1), 103–113. https://doi.org/10.1016/j.clpt.2005.10.002
Stresser, D. M., Perloff, E. S., Mason, A. K., Blanchard, A. P., Dehal, S. S., Creegan, T. P., Singh, R., & Gangl, E. T. (2016). Selective time-And NADPH-Dependent inhibition of human CYP2E1 by clomethiazole. *Drug Metabolism and Disposition*, *44*(8), 1424–1430. https://doi.org/10.1124/dmd.116.070193
Taavitsainen, P., Juvonen, R., & Pelkonen, O. (2001). In vitro inhibition of cytochrome P450 enzymes in human liver microsomes by a potent CYP2A6 inhibitor, trans-2-phenylcyclopropylamine (tranylcypromine), and its nonamine analog, cyclopropylbenzene. *Drug Metabolism and Disposition*, *29*(3), 217–222.
Tsai, M. C., & Gorrod, J. W. (1999). Determination of nicotine and its metabolites in biological fluids: in vitro studies. In *Analytical Determination of Nicotine and Related Compounds and their Metabolites*. Elsevier. https://doi.org/10.1016/b978-044450095-3/50016-4
Van Waateringe, R. P., Mook-Kanamori, M. J., Slagter, S. N., Van Der Klauw, M. M.,

Van Vliet-Ostaptchouk, J. V., Graaff, R., Lutgers, H. L., Suhre, K., El-Din Selim, M. M., Mook-Kanamori, D. O., & Wolffenbuttel, B. H. R. (2017). The association between various smoking behaviors, cotinine biomarkers and skin autofluorescence, a marker for advanced glycation end product accumulation. *PLoS ONE*, *12*(6), 1–15. https://doi.org/10.1371/journal.pone.0179330

von Bahr, C., Spina, E., Birgersson, C., Ericsson, Ö., Göransson, M., Henthorn, T., & Sjöqvist, F. (1985). Inhibition of desmethylimipramine 2-hydroxylation by drugs in human liver microsomes. *Biochemical Pharmacology*, *34*(14), 2501–2505. https://doi.org/10.1016/0006-2952(85)90533-7

Walsky RL, Obach RS, Gaman EA, Gleeson JP, Proctor WR. Selective inhibition of human cytochrome P4502C8 by montelukast. Drug Metab Dispos 2005;33:413-8.

Wang, P.-F., Neiner, A., & Kharasch, E. D. (2019). Efavirenz Metabolism: Influence of Polymorphic CYP2B6 Variants and Stereochemistry. *Drug Metabolism and Disposition: The Biological Fate of Chemicals*, *47*(10), 1195–1205. https://doi.org/10.1124/DMD.119.086348

Yamanaka, H., Nakajima, M., Fukami, T., Sakai, H., Nakamura, A., Katoh, M., Takamiya, M., Aoki, Y., & Yokoi, T. (2005). CYP2A6 and CYP2B6 are involved in nornicotine formation from nicotine in humans: Interindividual differences in these contributions. *Drug Metabolism and Disposition*, *33*(12), 1811–1818. https://doi.org/10.1124/dmd.105.006254

Yamanaka, H., Nakajima, M., Nishimura, K., Yoshida, R., Fukami, T., Katoh, M., & Yokoi, T. (2004). Metabolic profile of nicotine in subjects whose CYP2A6 gene is deleted. *European Journal of Pharmaceutical Sciences*, *22*(5), 419–425. https://doi.org/10.1016/j.ejps.2004.04.012

Yildiz, D. (2004). Nicotine, its metabolism and an overview of its biological effects. *Toxicon*, *43*(6), 619–632. https://doi.org/10.1016/j.toxicon.2004.01.017

Yokota, H., Ohgiya, N., Ishihara, G., Ohta, K., & Yuasa, A. (1989). Purification and properties of UDP-glucuronyltransferase from kidney microsomes of β-naphthoflavone-treated rat. *Journal of Biochemistry*, *106*(2), 248–252. https://doi.org/10.1093/oxfordjournals.jbchem.a122839

Zhou, Y., Ingelman-Sundberg, M., & Lauschke, V. M. (2017). Worldwide Distribution of Cytochrome P450 Alleles: A Meta-analysis of Population-scale Sequencing Projects. *Clinical Pharmacology and Therapeutics*, *102*(4), 688–700. https://doi.org/10.1002/cpt.690

Zhu, A. Z. X., Zhou, Q., Cox, L. S., Ahluwalia, J. S., Benowitz, N. L., & Tyndale, R. F. (2013). Variation in Trans-3'-Hydroxycotinine Glucuronidation Does Not Alter the Nicotine Metabolite Ratio or Nicotine Intake. *PLoS ONE*, *8*(8), 1–7. https://doi.org/10.1371/journal.pone.0070938

DMD Fast Forward. Published on February 23, 2022 as DOI: 10.1124/dmd.121.000624
This article has not been copyedited and formatted. The final version may differ from this version.

Footnotes

This work was supported by the National Institutes of Health, National Institutes of Environmental Health Sciences [Grant R01-ES025460] to P. Lazarus, the Fulbright-Garcia Robles Program and a CONACyT dissertation grant to Y.X. Perez-Paramo, and the Health Sciences and Services Authority of Spokane, WA [Grant WSU002292] to WSU College of Pharmacy and Pharmaceutical Sciences

Financial Disclosure: No author has an actual or perceived conflict of interest with the contents of this article.

DMD Fast Forward. Published on February 23, 2022 as DOI: 10.1124/dmd.121.000624
This article has not been copyedited and formatted. The final version may differ from this version.

Figure Legends

Figure 1. Schematic of the cotinine metabolism pathway. (1) nicotine, (2) COT, (3) 3HC, (4) COX, (5) COT-glucuronide, and (6) norcotinine. Percentages [taken from (Rangiah et al., 2011)] indicate the levels of each metabolite as a percentage of total cotinine metabolites in the urine from smokers.

Figure 2. COX detection by MS/MS and inhibition in pooled HLM. Panel A, representative UHPLC-MS/MS traces of COX formation. Top panel, COT (retention time = 1.06 min, mass transition m/z: 177.103 > 98); middle panel, COX (retention time = 1.80 min, mass transition m/z: 193.1 > 96); bottom panel, deuterium (D_3)-labeled COX (retention time = 1.80 min, mass transition m/z: 196.1 > 96). Panel B, specific inhibition of CYP450-mediated COT metabolism in pooled HLM. Data represent means of triplicate independent assays. *$p < 0.05$ as compared to incubations without inhibitor.

Figure 3. Kinetic analysis of COX formation in CYP450-overexpressing cell lines. Michaelis–Menten curves for microsomes of HEK293 cells overexpressing CYP2A6 (panel A), CYP2B6 (panel B), CYP2C19 (panel C), CYP2E1 (panel D) and CYP3A4 (panel E); and HLM (panel F). Each curve is representative of one of three different experiments. For cell line microsomes, the rate of COX formation was adjusted per mg of microsomal protein normalized based on V5 expression (determined using a V5 antibody) and on calnexin expression as determined by Western blot as described in the Materials and Methods.

DMD Fast Forward. Published on February 23, 2022 as DOI: 10.1124/dmd.121.000624
This article has not been copyedited and formatted. The final version may differ from this version.

Figure 4. CYP2C19 genotype-phenotype analysis in human liver specimens. Panel A, COX formation in specimens stratified by CYP2C19 genotypes (UM_{2C19}, EM_{2C19}, IM_{2C19} and PM_{2C19}; n= 113). Panel B, COX formation in specimens stratified by combined CYP2C19 genotypes (UM_{2C19}/EM_{2C19} vs. IM_{2C19}/PM_{2C19}). Panel C, the ratio of COX/3HC in specimens stratified by CYP2C19 genotypes (UM_{2C19}, EM_{2C19}, IM_{2C19} and PM_{2C19}). Panel D, the ratio of COX/3HC in specimens stratified by combined CYP2C19 genotypes (UM_{2C19}/EM_{2C19} vs. IM_{2C19}/PM_{2C19}). Genotype classifications are described in the Materials and Methods. KW test, Kruskal-Wallis test. *p = 0.017, **p < 0.01

DMD Fast Forward. Published on February 23, 2022 as DOI: 10.1124/dmd.121.000624
This article has not been copyedited and formatted. The final version may differ from this version.

Table 1. Kinetic analysis of cotinine-*N*-oxide formation by CYP450 enzymes.

CYP enzyme	K_M (uM)[a]	V_{max} (pmol • min^{-1} • mg^{-1})[a, b]	V_{max}/K_M (nL • min^{-1} • mg^{-1})[a, b]
2A6	390 ± 87	17 ± 1.5	44 ± 7.6
2B6	810 ± 24	16 ± 0.01	22 ± 6.9
2C19	405 ± 19	15 ± 1.6	42 ± 19
2E1	> 10 mM	ND[d]	ND
3A4	> 10 mM	ND	ND
HLM[c]	550 ± 49	587 ± 26	1070 ± 8.4

[a] Data are expressed as the mean ± S.D. of three independent experiments. Cotinine concentrations of 0.005-10 mM were used for kinetic analysis.

[b] The V_{max} was calculated per total microsomal protein levels after normalization based on microsomal CYP expression levels as determined by Western blot analysis.

[c] Pooled human liver microsomes (HLM) from 20 individuals.

[d] ND, not determined

DMD Fast Forward. Published on February 23, 2022 as DOI: 10.1124/dmd.121.000624
This article has not been copyedited and formatted. The final version may differ from this version.

Table 2. Rate of COX and 3HC production in HLM specimens.[a]

	Mean ± SD[b] (pmol•min^{-1}•mg^{-1})	Range (pmol•min^{-1}•mg^{-1})
COX	11.8 ± 6.4	0.71 - 31.2
3HC	28.1 ± 14.9	3.4 - 101

[a] n=113 HLM specimens.
[b] SD, standard deviation.

Figure 1

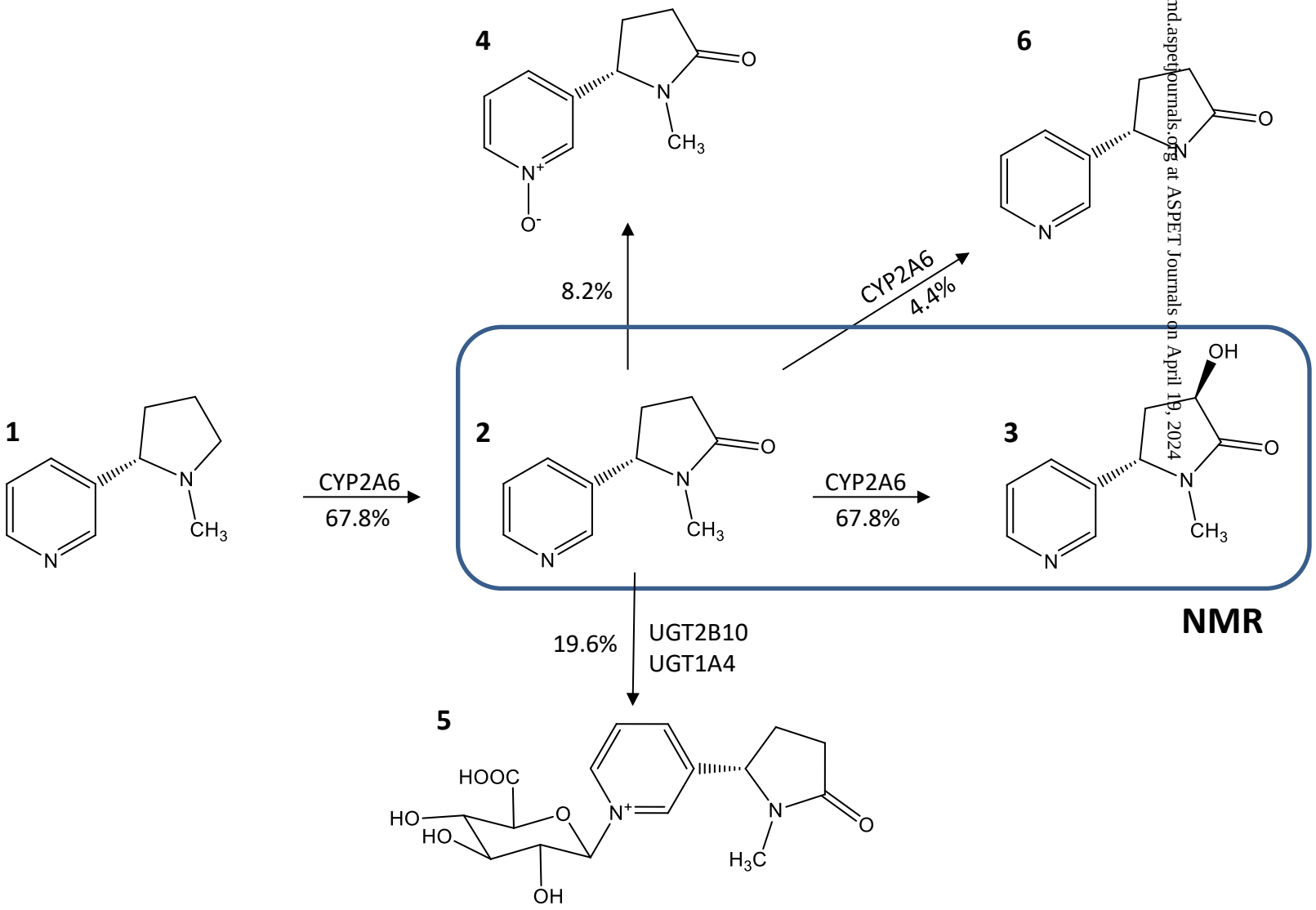

Figure 2

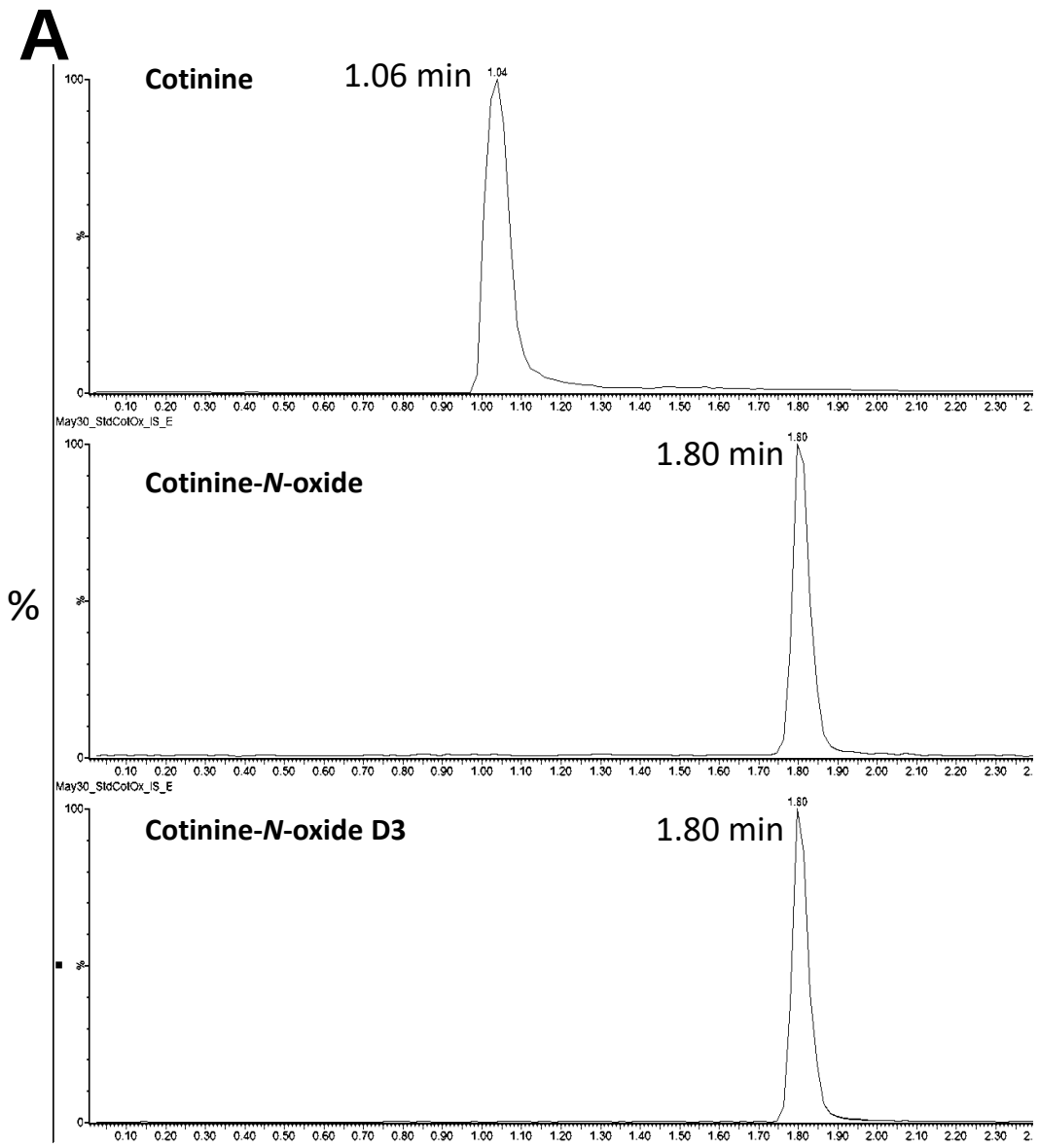

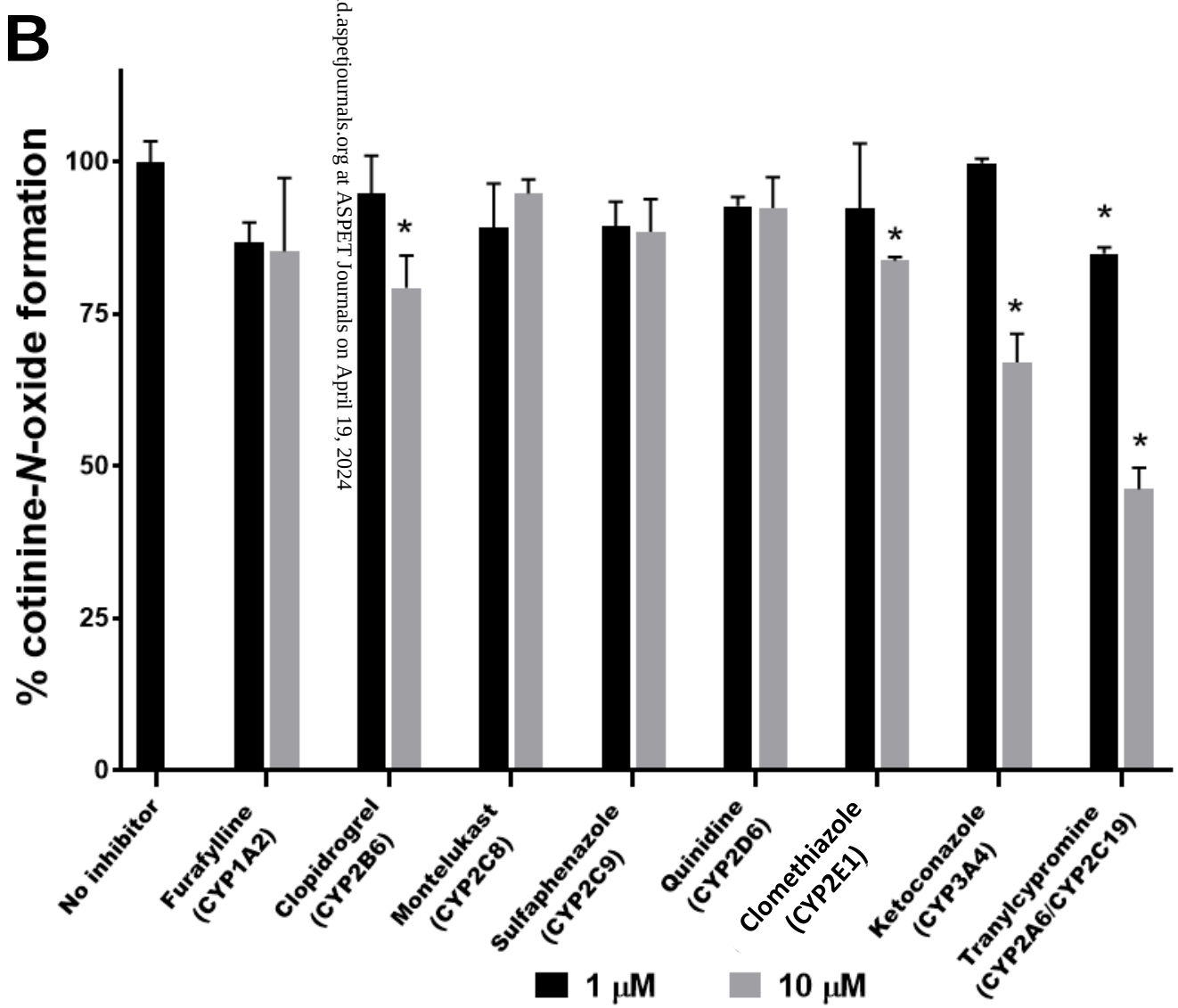

Figure 3

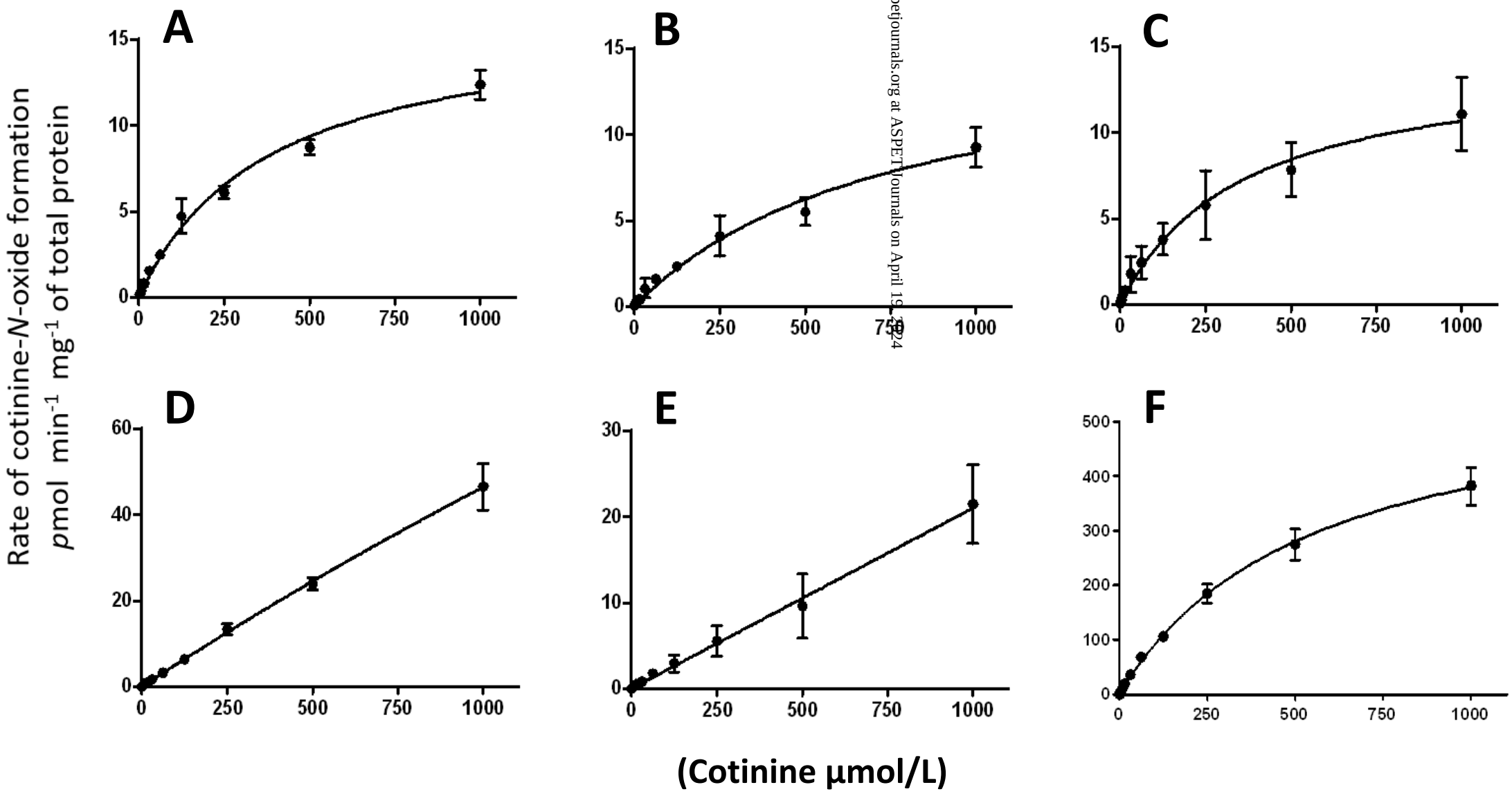

Figure 4